Recent Results from RHIC & Some Lessons for Cosmic-Ray Physicists

Spencer R. Klein[a] *

[a]Nuclear Science Division, Lawrence Berkeley National Laboratory, Berkeley, CA, 94720, USA

The Relativistic Heavy Ion Collider (RHIC) studies nuclear matter under a variety of conditions. Cold nuclear matter is probed with deuteron-gold collisions, while hot nuclear matter (possibly a quark-gluon plasma (QGP)) is created in heavy-ion collisions. The distribution of spin in polarized nucleons is measured with polarized proton collisions, and photoproduction is studied using the photons that accompany heavy nuclei.

The deuteron-gold data shows less forward particle production than would be expected from a superposition of pp collisions, as expected due to saturation/shadowing. Particle production in AA collisions is well described by a model of an expanding fireball in thermal equilibrium. Strong hydrodynamic flow and jet quenching shows that the the produced matter interacts very strongly. These phenomena are consistent with new non-perturbative interactions near the transition temperature to the QGP.

This writeup will discuss these results, and their implications for cosmic-ray physicists.

Since the first collisions in 2001, RHIC has produced a wealth of data on pp, dAu, AuAu and CuCu collisions at center of mass energies from 20 to 200 GeV per nucleon pair. RHIC was built to study aspects of QCD; the main foci have been the study of cold nuclear matter via dA collision, and of hot nuclear matter (the Quark Gluon Plasma (QGP)?), via heavy-ion collisions. RHIC also studies polarized proton collisions to measure the polarized parton distributions, and photonuclear interactions. This data is also of interest for modelling cosmic-ray air showers.

RHIC hosts 5 experiments. There are two large experiments, PHENIX and STAR, and 3 smaller ones: PHOBOS, BRAHMS and pp2pp.

PHENIX has two large central spectrometers, and a forward muon system [1]. It is optimized for particle identification, particularly for leptons.

STAR is optimized for global event studies, with a large acceptance time projection chamber for charged particles and a calorimeter to detect neutral particles [2].

PHOBOS detects charged particles over a very large pseudorapidity range, $|\eta| < 5.4$, and has two small spectrometer arms for tracking [3]. Pseudorapidity $\eta = -\ln[\tan(\theta/2)]$, where θ is the angle between the particle direction and the beam axis. BRAHMS consists of central and forward spectrometers, with precise particle tracking and identificaton in a small solid angle [4]. pp2pp consists of Roman pots which track protons scattered at small angles; it studies pp diffraction [5].

This writeup will review the different RHIC physics, starting with polarized proton collisions and photoproduction, before moving on to discuss cold and hot nuclear matter.

1. pp and Polarized Proton Collisions

pp collisions serve two functions at RHIC: tests of pQCD calculations with unpolarized pp collisions, and measurements of the polarized parton distributions.

Jet and single particle cross section data at RHIC are in good agreement with recent perturbative QCD calculations [6,7]. Figure 1 compares pQCD calculations with data for π^0 cross sections; the agreement is good. This good agreement is possible thanks to recent next-to leading order pQCD calculations and improved fragmentation functions.

Polarized proton collisions are used to study the spin structure of the nucleon [8]. The total nucleon spin is the sum of the quark spins, gluon spins and orbital angular momentum within the proton. Experiments at SLAC and CERN in the 1970s-1990s showed that the quarks carry a relatively small fraction of the nucleon spin; this is

*Email: srklein@lbl.gov

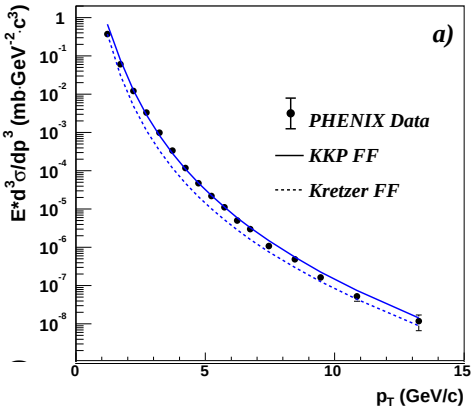

Figure 1. PHENIX data on π^0 production in in 200 GeV pp collisions, compared with NLO pQCD calculations plus two different fragmentation functions [6].

sometimes called the 'spin crisis.' RHIC will measure the gluon polarization, via quark-gluon and gluon-gluon interactions. The polarized gluon distributions are found by comparing the normalized rates for collisions where the proton spins are pointing in the same vs. in opposite directions, Although much more data is needed, already it is possible to exclude the most extreme models of gluon polarization [7].

2. Photoproduction

Photoproduction has been studied in gold-gold and deuteron-gold collisions. Virtual photons from the electromagnetic field of one nucleus interact with the other nucleus. Photoproduction of the J/ψ is sensitive to the gluon distributions of the target nucleus [9]. ρ and $\pi^+\pi^-\pi^+\pi^-$ final states have also been studied [10].

Vector meson photoproduction can occur two ways: nucleus 1 can emit a photon which interacts with nucleus 2, or vice-versa. The two channels are indistinguishable, so they interfere. Going from one emitter to the other is a parity inversion, and vector mesons are negative parity, so the two amplitude subtract. At mid-rapidity

$$\sigma(b) = \sigma_0(b)(1 - \cos(p_T \cdot b)). \quad (1)$$

Here, σ_o is the cross section without interference the p_T is that of the vector meson, and b is the impact parameter (distance between the two ion centers at closest approach). b is not an observable, so the total cross section is the integral of Eq. 1. This interference has been observed through a reduction in cross section for $p_T < \hbar/\langle b \rangle$ [11].

Because of the strong nuclear fields, some reactions can uniquely be studied in heavy-ion collisons. At RHIC, multi-photon interactions involving a single ion pair *i.e.* $Au + Au \rightarrow Au^* + Au^* + \rho$ via 3 photon exchange (one for each nuclear exchange, and a 3rd to produce the ρ^0) has also been studied [10]. The LHC will reach γp center of mass energies up to several hundred GeV, well beyond the reach of HERA [12].

3. Cold Nuclear Matter

By comparing pp and dA collisions the effects of the nuclear environment may be studied. The nuclear environment is expected to alter parton densities, possibly leading to qualitatively new behavior [13]. Gluons have a virtuality (Q^2) dependent transverse area $\pi(\hbar c)^2/Q^2$. At high densities (i.e. at low x), partons will recombine, in reactions like $g+g \rightarrow g$. This recombination moderates the growth in gluon density as x decreases. Because of the higher parton density, recombination is more significant in nuclei, and comparisons of parton distributions in protons and in nuclei are sensitive to these changes; the difference measured in lepton-nucleon interactions is known as shadowing.

Figure 2 shows the effect of this density on particle production. It compares charged-particle production in dAu and pp collisions at different pseudorapidity [14]. Higher pseudorapidity corresponds to higher-x partons from the deuteron, and lower-x partons from the gold; as expected from recombination, shadowing is larger at lower-x.

Different theoretical studies have used BFKL and/or DGLAP evolution, or taken advantage of

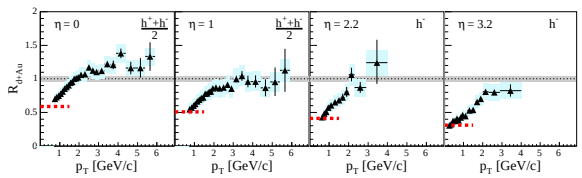

Figure 2. The ratio of charged particle production in dA and pp collisions (normalized to the number of nucleon-nucleon collisions) at different pseudorapidity. In the absence of nuclear effects, R_{dAu} should equal 1. [14].

the relationship between shadowing and diffraction. One interesting new approach, the colored glass condensate (CGC) treats the gluon fields in the nucleus as a classical field.

The CGC makes some interesting predictions [15]; a CGC should interact coherently as a single object, producing some new effects. When a parton interacts with a CGC, the CGC recoils coherently; because of it's high mass, the recoil is muted, leading to apparent 'monojets'. Without a CGC, 2 parton → 2 parton reactions like $g + g \rightarrow g + g$ produce two azimuthally back-to-back jets. However, if the gluon strikes a CGC, the heavy object will recoil slowly, and the recoiling gluon will produce the single visible jet. This process is studied experimentally via 2-particle correlations. Figure 3 shows the azimuthal angle correlations between a π^0 produced in the forward direction and a charged hadron produced near mid-rapidity, for pp and dA collisions. Dijet events should produce back-to-back correlations. These correlations are smaller for dA collisions than for pp collisions, as expected from CGC models. The suppression rises at smaller π^0 energies, as expected from a CGC.

4. Hot Nuclear Matter

A main experimental goal of RHIC is to search for the quark gluon plasma (QGP), an interacting system of partons in equilibrium [17]. Lattice gauge theory predicts that a QGP is produced

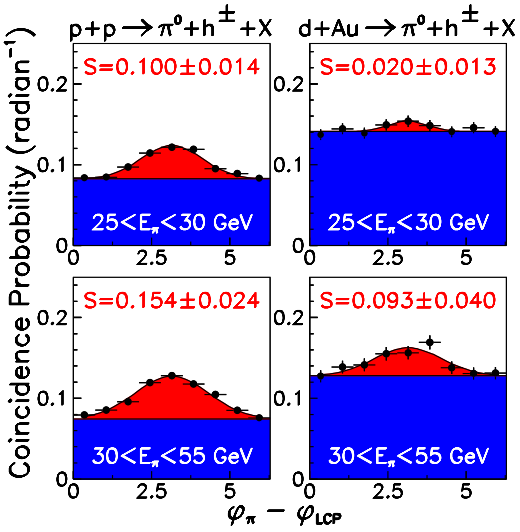

Figure 3. Azimuthal correlations between a forward π^0 and a more central charged hadron in (left) pp and (right) dA collisions for (top) $25 < E_\pi < 30$ GeV and (bottom) $30 < E_\pi < 55$ GeV [16]. The lower (blue) area shows the background, while the higher (red) area follows a fit to the data (points). The 'S' values give the size of the peak, smaller in dA collisions. The correlations are expected in dijet events.

when nuclear matter at low baryochemical potential (baryon density) is heated to a temperature above about 170 MeV [18].

RHIC heats nuclear matter by colliding heavy ions. The collisions occur in several stages. Initially, the ions collide and their partons interact, producing new partons. These partons themselves interact, producing still more partons. As these interactions occur, the system expands and cools. Eventually, the partons form hadrons which may themselves interact. Interactions continue until the system cools enough that no further inelastic processes are possible; this transition is known as chemical freezeout. Later, the hadrons separate enough that no further elastic collisions occur; this is thermal freezeout.

Much RHIC data is analyzed in terms of cen-

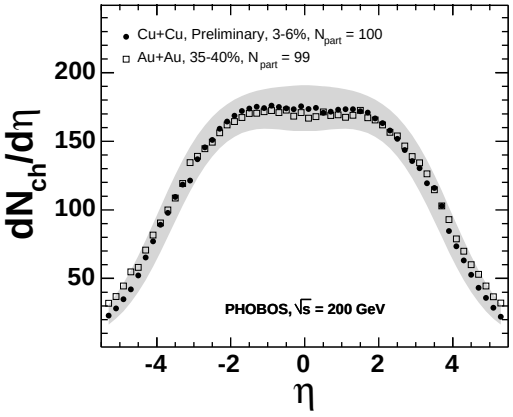

Figure 4. $dN/d\eta$ for $3-6\%$ copper-copper collisions and $35-40\%$ gold-gold collisions. The two datasets have very similar N_{part}, and almost identical $dN/d\eta$ [19].

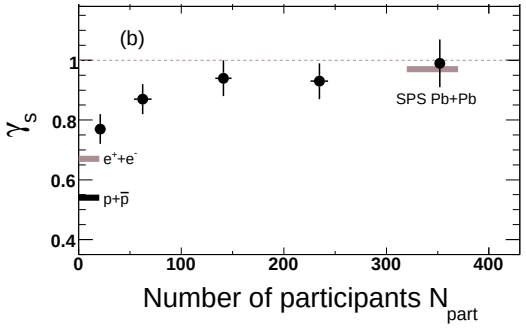

Figure 5. Strangeness suppression factor γ_s as a function of N_{part}. π, K, p, Λ, ξ and Ω particles and their antiparticles were used to determine γ_s [20].

trality, or impact parameter (b). Several methods are used to characterize centrality: N_{part} is the number of nucleons participating in the collision; for a head-on collision, $N_{part} = 2A$. N_{bin} is the number of binary (nucleon-nucleon) collisions; this is relevant for comparing pQCD participle production between pp and AA collisions. For a given b, N_{part} and N_{bin} are determined using a Glauber calculation. Centrality is also given in percentages, such as the $0-10\%$ most central collisions.

4.1. Overall Event Structure

We begin by considering the particle production. Figure 4 compares the pseudorapidity (η) distribution for $3-6\%$ central copper-copper collisions with $35-40\%$ gold-gold collisions; the two datasets have almost identical N_{part}. At least for identical nuclei, N_{part} determines the collision dynamics. It can be used to model other systems, such as collisions involving nitrogen.

The final state composition is well described by a thermal model, with production at an equilibrium temperature of $T_c = 165 \pm 10$ MeV; The abundance of particle species x, N_x depends on its mass m_x [20]:

$$N_x \approx exp(-m_x/kT_c). \quad (2)$$

In contrast to pp collisions, strangeness is fully equilibrated; there is no strangeness suppression. The system is described by a grand-canonical ensemble; a large thermal bath conserves strangeness, and individual strange particles can be produced, rather than the pairs required in smaller systems. Figure 5 shows how the strangess suppression factor γ_s varies with N_{part}. Here, $\gamma_s = 1$ corresponds to thermal equilibrium, Eq. (2). For pp collisions, $\gamma_s \approx 0.54$. Strangeness production is enhanced over pp collisions even for relatively small systems, such as nitrogen-nitrogen collisions. For heavy systems, the strangness content almost doubles.

A more detailed model of the collision includes both thermal energy of collective expansion, *i.e.* a hydrodynamically expanding fireball. The 'blast wave' model describes this hydrodynamic expansion with two parameters: system temperature, T and a collective expansion velocity, $\langle\beta\rangle$, the velocity at the outer edge of the fireball [21]. Different velocity profiles can be used, with small effects on the final results. Because of the collective expansion, heavier particles have higher $\langle p_T\rangle$. Fits to the p_T spectra of different particles find $T \approx 106$ MeV, and $\langle\beta\rangle \approx 0.55$c. This model has been fit

to a large body of RHIC data, with considerable success [21]. It described soft-particle production in ion collisions, and might be of use for simple air-shower simulations.

Elliptical flow is another aspect of the hydrodynamical behavior of the system. In a non-central heavy-ion collision, the overlap region is roughly almond shaped. Pressure converts this spatial anisotropy into a particle density anisotropy. The particle flux depends on ϕ, the azimuthal (perpendicular to the beam) angle with respect to the reaction plane (line between the centers of the two nuclei). The dependence is

$$\frac{dN}{d\phi} = 1 + 2v_2 \cos(2\phi) + ... \quad (3)$$

The elliptical flow, v_2 varies with particle species and p_T. Additional terms for directed flow (e.g. v_1) and a small quadrupole moment are ignored here. Hydrodynamic flow is a powerful diagnostic tool, since it probes particle interactions (e.g. pressure) very early in the collision. At low momenta, $p_T < 2$ GeV, the measured particle flow is consistent with hydrodyamic models. The initial-state spatial anisotropy is completely converted into a particle asymmetry. Nuclear matter acts like a nearly perfect fluid.

Figure 6 shows the elliptic flow per constituent quark, v_2/n ($n = 2$ for mesons; $n = 3$ for baryons), as a function of p_T per constituent quark, for a variety of different particles. Except for pions, all of the baryon and meson data lie near a single line, with very similar per-quark flow [22]. It appears that partons are flowing, rather than hadrons. Proposed explanations for the higher pion v_2 include their low mass, and/or feed-down from decays of heavier resonances. Still, the v_2 data shows fairly clearly that the early interactions involve partons, rather than hadrons.

A final characteristic of the overall event is the system size at thermal freezeout. This is determined using Hanbury-Brown Twiss (HBT) interferometry, a measurement of the system size that relies on the enhancement in boson (π, etc.) production at small momentum differences, $|\vec{p}_1 - \vec{p}_2| < \hbar/R$. By measuring the increased particle production at small momentum differences, the source size can be inferred. At freezout (last interaction), central gold-gold collisions have a Gaussian radius of about 6 fm, about twice the size of the original system.

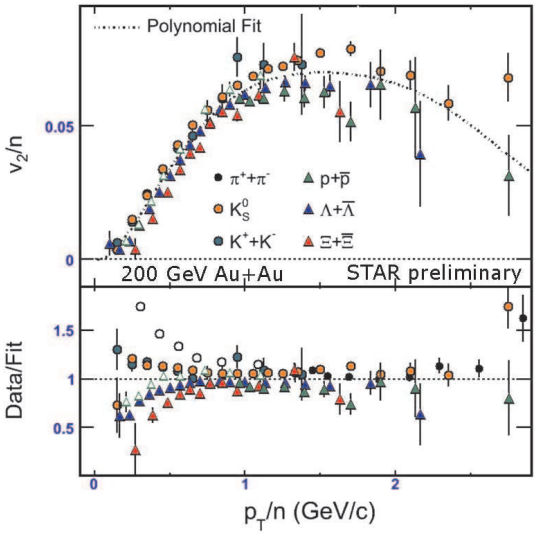

Figure 6. Elliptic flow per constituent quark, v_2/n, (n being the number of constituent quarks in the hadron) vs. p_T/n for various hadrons. Except for the π, the flow of both mesons and baryons follows a very similar line, indicating that quarks flow, rather than hadrons [22].

4.2. Perturbative Probes of the QGP

Other studies of the QGP use high p_T probes produced in the collisions. High p_T particle production is well described by pQCD. Except for some relatively minor nuclear effects, high p_T (usually $p_T > 2$ GeV/c) particle production should be the same in pp, pA and AA collisions, described by initial state parton distributions, pQCD, and universal fragmentation functions. Any large differences between systems should be due to the interactions between the produced particles and the nuclear medium. The time scale for fragmentation (whereby partons fragment into hadronic jets) is relatively long compared to the time a parton remains in the fireball, so medium

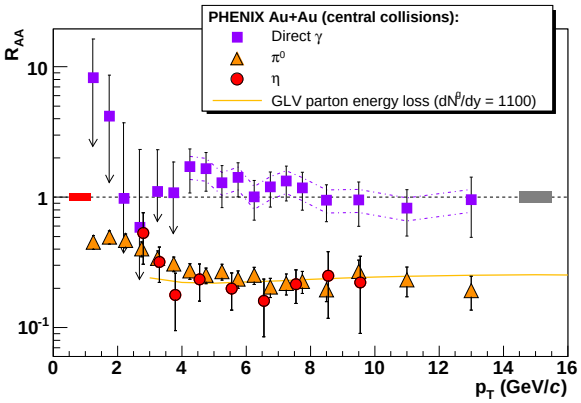

Figure 7. R_{AA} for π^0, η and direct photons, together with a theoretical calculation of energy loss for a plasma with a gluon density of 1100 gluons/unit of rapidity [24]. Hadrons with a color charge are heavily suppressed; photons are not.

interactions should involve the produced parton, rather than the final-state hadrons. Energy loss in the medium will manifest itself as a reduction in high p_T particle production as energetic particles are shifted to lower p_T. This reduction is measured by comparing spectra from central AA collisions with appropriately scaled pp and/or peripheral AA collisions, using the ratio

$$R_{AA} = \frac{\sigma_{AA}}{N_{bin}\sigma_{pp}}. \quad (4)$$

In the absence of nuclear effects, $R_{AA} = 1$. Figure 7 shows R_{AA} for π^0, η and direct γ. For direct photons $R_{AA} \approx 1$; photons do not interact with the medium. However, for both types of hadrons, $R_{AA} \approx 0.2$ for $2 < p_T < 20$ GeV/c, showing a large nuclear suppression. In dAu collisions (not shown here), $R_{AA} \approx> 1$, as expected due to initial state parton scattering.

In perturbative QCD, the suppression depends on the parton density in the fireball and the parton-parton cross section. For the standard pQCD cross sections, the observed energy loss requires a parton density of 1100-1200 gluons/unit of rapidity [25]. This is far higher than the density inferred from the final state multiplicity.

R_{AA} has also been measured for heavy quarks. Since heavy quarks have a lower velocity (for a given momentum) than lighter quarks, less radiative energy loss is expected. However, R_{AA} for heavy quarks is similar to that for light quarks [26]. This is difficult to understand in any pQCD calculation.

R_{AA} has also been measured for the J/ψ. For central AuAu collisions, $R_{AA} \approx 0.3$ [27]. This is integrated over all p_T, so is not directly comparable to the other R_{AA} measurements. The suppression is comparable to what was seen at $\sqrt{s_{NN}} = 17.3$ GeV at the CERN SPS; this energy independence is somewhat surprising.

Parton energy loss can also be studied with particle correlations. A high p_T particle is selected as a 'trigger' particle, and the azimuthal correlation with a lower p_T 'associated' particle studied. Figure 8 compares the azimuthal correlations for dA and for mid-peripheral and central $AuAu$ collisions, for trigger particles with $p_T > 8$ GeV/c and different p_T associated particles. The dAu data has a narrow peak for $\Delta\phi \approx 0$ (near-side) and a slightly broader peak for $\Delta\phi \approx \pi$ (far-side). The former is from same-jet correlations, while the latter is from correlations involving two back-to-back jets; the pp data (not shown) has a similar structure. The mid-peripheral $AuAu$ data has a similar behavior, although with higher backgrounds. In central $AuAu$ collisions, the back-to-back peak is much smaller, especialy for softer associated particles. The near-side ($\Delta\phi \approx 0$) peak is largely unchanged. For softer trigger particles, the far-side peak largely disappears.

This data fits a model where the high p_T particles come from parton interactions near the surface of the fireball. Partons produced deeper in the fireball lose most of their energy by dE/dx, and so do not produce high p_T hadrons. High p_T partons produced near the surface, pointing outward produce full-scale jets, with 'normal' near-side correlations. The suppression factor R_{AA} depends on the surface to volume ratio of the system. Back-to-back jets occur only for a narrow range of geometries, where a near-surface interaction produces back-to-back partons nearly tangential to the surface.

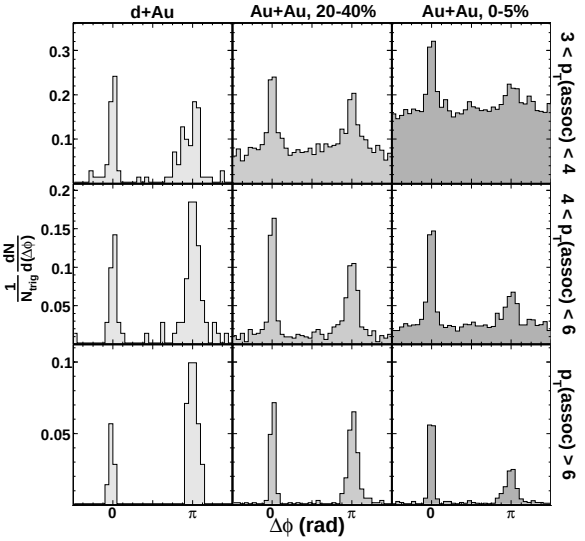

Figure 8. Azimuthal correlations between a trigger particle with $p_T > 8$ GeV/c and an associated particle in different p_T ranges (in GeV/c) for dAu and mid-peripheral and central $AuAu$ collisions [28].

5. Recent Theoretical Developments

The blast wave model does an excellent job of modelling soft particle production at RHIC. However, the fit parameters imply very high interaction cross sections; these cross sections do not agree with expectations from pQCD based particle interactions. Several related puzzles are also of interest:

1) The elliptic flow is at the hydrodynamic limit, with the produced matter behaving like an almost perfect fluid.

2) The R_{AA} measured at high p_T can only be explained in a pQCD framework by an unphysically high local parton density.

3) The R_{AA} for heavy quarks is similar to that for lighter particles.

These puzzles have led to considerable theoretical speculation. Ed Shuryak has proposed that the temperature range $T_C < T < 4T_c$ is a strongly coupled regime for partons [29]; In this non-perturbative phase, there are many very weakly bound colored states/resonances, such as qq, gg, qqg, etc. These states are very lightly bound, so have large radii, leading to rescattering cross sections 10 to 100 times those predicted by pQCD. Similar behavior is seen for atoms that have been tuned (via a magnetic field) to be barely bound. Shuryak also pointed out that this strongly coupled QGP (sQGP) may be expected based on duality arguments with weakly coupled string theory. At the same time, lattice calculations indicate that meson bound states (notably including the J/ψ surrvive up to temperatures considerably above $\approx 1.5T_c$; this could explain the lack of additional suppression.

These strong interactions may explain the large elliptic flow and reduced R_{AA}. The strong interactions could also reduce the QGP lifetime (as is seen in some HBT studies). In short, this strongly-coupled phase could explain many of these puzzling observables. Of course, detailed quantitative studies are needed.

One measure of the cross section is the fluid viscosity; elliptic flow depends on the shear viscoity/entropy (η/s). Flow data shows $\eta/s < 0.1$ [30], indicating that the sQGP is a 100 times better fluid than water. This viscosity is much lower than that expected for a hadron gas or from a perturbative (i.e. hotter) QGP, and appears beyond the reach of perturbative QCD. In fact, it approaches the quantum limit, $\eta/s \approx 1/4\pi$, calculated using duality arguments [30].

6. Lessons for Cosmic-Ray Modelling

RHIC data offers some guidance for modelling cosmic-ray air showers. Nuclear effects are significant; AA collisions are not merely superpositions of pp or even pA collisions. A blast-wave model does a good job of explaining soft particle production; it may be of interest for simple simulations. Three aspects of the RHIC data that may be particularly significant are:

1) The reduced forward particle production in dA collisions may be due to decreased parton densities in nuclei at low x. This may reduce number of high energy muons, and/or affect the downward energy flow in air showers. More quantita-

tive saturation models are needed to model higher energy interactions.

2) The strangenss content in nuclear collisions is significantly increased over pp collisions even at moderate N_{part}, in pA and AA, and, probably, in πA collisions. At RHIC energies, the increase is about 50% for nitogren-nitrogen collisions. Since $K^{\pm}$ decay faster than $\pi^{\pm}$, in air showers, they are more likely to decay before interacting, so the increased strangeness should lead to more high energy muons. The increased strangeness will also reduce the π^0 fraction in collisions, slowing the conversion of hadronic energy into electromagnetic energy. This may partially counterbalance the previous item.

3) Lighter systems may be modelled by using the N_{part} dependence of heavy-ion systems.

7. Conclusions and Future Prospects

A simple explosive-exansion model can explain much of the soft particle production data. Similarly, a surface emission picture can explain a lot (but not all) of the high p_T particle production. However, pQCD calculations do not reproduce the parameters required for these models. It may be that a new non-perturbative QGP is being produced at RHIC energies.

Over the next few years, the RHIC detectors will upgrade their subsystems. The major experimental goals are high-statustics studies of open charm and Υ production and of leptonic decays of vector mesons; the latter may be sensitive to chiral symmetry breaking. Another interesting idea is to search for the tricritical point of QCD; this might be found at non-zero baryon density; RHIC can search for it point by scanning the machine energy.

I thank the organizers for an enjoyable meeting, and my RHIC colleagues for useful suggestions. This work was supported by the U.S. DOE under contract number DE-AC03076SF00098.

REFERENCES

1. K. Adcox *et al.*, Nucl. Instrum. & Meth. **A499**, 469 (2003).
2. K. H. Ackermann *et al.*, Nucl. Instrum. & Meth. **A499**, 624 (2003).
3. B. B. Back *et al.*, Nucl. Instrum. & Meth. **A499**, 603 (2003).
4. M. Adamczyk *et al.*, Nucl. Instrum. & Meth. **A499**, 437 (2003).
5. S. Bultmann *et al.*, Nucl. Instrum. & Meth. **A535**, 415 (2003).
6. S. S. Adler *et al.*, Phys. Rev. Lett. **91**, 241803 (2003).
7. B.I. Abelev *et al.*, hep-ex/0608030; S. S. Adler *et al.*, Phys. Rev. **D73**, 091102(R), (2006).
8. G. Bunce *et al.* Ann. Rev. Nucl. Part. Sci. **50**, 525 (2000).
9. J. Nystrand, hep-ph/0611042.
10. S. Klein, nucl-ex/0506013.
11. S. Klein, nucl-ex/0402007
12. C. A. Bertulani *et al.*, Ann. Rev. Nucl. Part. Sci. **55**, 271 (2005); G. Baur *et al.*, Phys. Rept. **364**, 359 (2002).
13. L. Frankfurt, M. Strikman and C. Weiss, Ann. Rev. Nucl. Part. Sci. **55**, 403 (2005).
14. I. Arsene *et al.*, Phys. Rev. Lett. **93**, 242303 (2004).
15. E. Iancu and R. Venugopalan, hep-ph/0303204.
16. J. Adams *et al.*, Phys. Rev. Lett. **97**, 152302 (2006).
17. D. d'Enterria, nucl-ex/0611012.
18. F. Karsch, hep-lat/0601013.
19. G. Roland, in *Proc. Quark Matter 2005.*
20. J. Adams *et al.*, nucl-ex/0606014.
21. F. Retiere and M. Lisa, Phys. Rev. **C70**, 044907 (2004).
22. R. Lacey, nucl-ex/0510029.
23. J. Adams *et al.*, Phys. Rev. **C71**, 044906 (2005); S.S. Adler *et al.*, Phys. Rev. Lett. **93**, 152302 (2004).
24. S.S.Adler *et al.*, Phys. Rev. Lett. **96**, 202301 (2006).
25. I. Vitev and M. Gyulassy, Phys. Rev. Lett. **89**, 252301 (2002).
26. S. S. Adler *et al.*, Phys. Rev. Lett. **96**, 032301 (2006); B. I. Abelev *et al.*, nucl-ex/0607012.
27. M. Leitch, nucl-ex/0607010.
28. J. Adams *et al.*, nucl-ex/0604018.
29. E. V. Shuryak, hep-ph/0405066.
30. D. Teaney, Phys. Rev. **C68**, 034913 (2003).